


Article

A Biophysical Framework for High-Intensity Laser Therapy Based on Photoacoustic Pressure Thresholds

Damiano Fortuna ¹, Fabrizio Margheri ², Scott Parker ³ and Francesca Rossi ^{4,*} ¹ Independent Researcher, 50100 Florence, Italy; fortuna.dami@gmail.com² El.En. Group, Via Baldanzese 17, 50041 Calenzano, Italy; f.margheri@elen.it³ DEKA Dental Lasers, 400 North Ashley Drive, Suite 2600, Tampa, FL 33602, USA; drsparker@gmail.com⁴ Institute of Applied Physics “Nello Carrara” (CNR-IFAC), Via Madonna del Piano 10, 50019 Sesto Fiorentino, Italy

* Correspondence: f.rossi@ifac.cnr.it

Abstract

High-Intensity Laser Therapy (HILT) represents a mechanistic subset of High-Power Laser Therapy (HPLT), distinguished by the addition of a photoacoustic component to established photochemical and photothermal effects. High-peak (kW), short-pulse emission generates pressure waves exceeding 10 kPa in water (27 °C) and approximately 100 kPa in vivo, levels that are compatible with the activation of mechanotransductive processes relevant to cellular differentiation. These pressure waves propagate several centimeters into biological tissues, extending beyond the optical penetration depth of light. We introduce Pulse Energy Dose (PED), a physically grounded and clinically oriented dose metric, to determine whether a laser system meets the photoacoustic threshold while remaining within the thermoelastic regime. Only systems combining kilowatt-range peak power, microsecond pulses, high pulse energy, and very low duty cycles (<1%) consistently induce pressure waves within the therapeutic thermoelastic regime. PED was validated against the Margheri equation, showing a strong linear correlation with calculated pressure wave amplitude (Pearson $r > 0.9$, $p < 0.0001$). Based on these results, we define operational bounds that identify high-power laser systems capable of producing reproducible photoacoustic effects within thermoelastic conditions. This framework shifts classification from average power to mechanism of action, providing guidance for safe parameter selection and supporting a mechanism-based clinical use of high-power lasers, particularly in musculoskeletal disorders, cartilage regeneration, bone healing, and deep-tissue repair.

Keywords: High-Intensity Laser Therapy; pulse energy dose; photoacoustic effects; thermoelastic regime; regenerative medicine



Academic Editors: Manuel Filipe Pereira da Cunha Martins Costa and Sandra Franco

Received: 22 October 2025

Revised: 18 December 2025

Accepted: 23 December 2025

Published: 3 January 2026

Copyright: © 2026 by the authors.

Licensee MDPI, Basel, Switzerland.

This article is an open access article distributed under the terms and conditions of the [Creative Commons Attribution \(CC BY\) license](https://creativecommons.org/licenses/by/4.0/).

1. Introduction

The therapeutic use of light in biology was first explored in the 1960s, when Endre Mester observed accelerated tissue regeneration following low-level laser exposure [1]. This pioneering discovery laid the foundation for photobiomodulation (PBM), later advanced by Tina Karu [2], who demonstrated that Cytochrome C oxidase absorbs red and near-infrared (NIR) light, enhancing ATP production and activating intracellular signaling pathways, such as PI3K/AKT and ERK/MAPK.

Subsequent work by Tunér and Hode [3] emphasized the relevance of wavelength, fluence, and pulse structure in determining therapeutic outcomes. More recently, in vitro studies by Sleep et al. [4] confirmed the biphasic cellular response to light: moderate

energy doses ($\sim 5.3 \text{ J/cm}^2$) enhance mitochondrial and osteogenic activity, whereas excessive exposure ($>10 \text{ J/cm}^2$) may inhibit these effects, particularly in the absence of mechanical stimulation.

Laser–tissue interactions occur through three primary biophysical mechanisms:

Photochemical effects, typical of LLLT, modulate mitochondrial function and inflammatory mediators (Lawrence & Sorra [5]).

Photothermal effects, predominant in HPLT, convert light into heat and promote vasodilation, extracellular matrix (ECM) remodeling, and transient analgesia [6–9]. Additional immunomodulatory effects have also been reported [10,11], along with immunomodulation (Mikhaylov et al. [10], Alghitany et al. [11]). However, if not carefully dosed, thermal stress may occur.

Photoacoustic effects, exclusive to HILT, result from high-peak, short-duration pulses generating acoustic pressure waves. These waves activate mechanotransduction via tyrosine kinase signaling (Tarantino et al. [12]) and cytoskeletal remodeling (Monici et al. [13] and Cialdai et al. [14]) and promote fibrocyte-to-fibroblast conversion [15,16], which are key steps in tissue repair.

Preclinical and clinical studies [17–20] show that HILT promotes deep-tissue regeneration, requiring pressure waves exceeding 10 kPa in water at 27 °C. Considering the higher absorption coefficients in vivo [21], this threshold increases to approximately 100 kPa. This value is consistent with the magnitude of mechanical stimuli reported in hypergravity studies [13,14,22–25].

Although the Margheri equation (Equation (2)) [26] accurately models these effects, its complexity limits clinical utility. Therefore, we propose the Pulse Energy Dose (PED, Equation (5)), a simplified yet biophysically sound parameter derived from the Pulse Intensity Fluence (PIF) model (Fortuna & Masotti [27]) to evaluate whether a laser system can generate therapeutic pressure waves.

This study introduces PED as the basis of a new mechanism-based classification of therapeutic lasers, distinguishing photoacoustic-capable HILT configurations from conventional systems by their ability to exceed photoacoustic thresholds within the thermoelastic regime.

In this framework, the pressure threshold discussed in this study should be interpreted as a physical and operational reference for the reliable generation of photoacoustic waves under thermoelastic conditions, rather than as a universal biological activation threshold applicable to all cell types or tissues.

1.1. Laser Systems Classification

Historically, laser therapy was first defined in the context of low-level laser therapy (LLLT), now referred to as photobiomodulation (PBM), which was initially characterized by average powers below 0.5 W and later extended to approximately 1 W. Subsequently, the term High-Intensity Laser Therapy (HILT) was introduced to describe a distinct class of high-power pulsed lasers designed to generate specific physical effects beyond purely photochemical and photothermal interactions. Over time, however, the term HILT has been increasingly used to describe a broad range of laser systems operating above the conventional LLLT power threshold, regardless of their underlying emission characteristics. As a result, high-power laser therapy (HPLT) currently encompasses heterogeneous systems with markedly different biophysical behaviors. In this context, the present study adopts a mechanistic definition of HILT, identifying it as a specific subset of high-power laser systems capable of generating reproducible thermoelastic photoacoustic pressure waves.

LLLT operates at average powers below 1 W and induces photochemical effects. It is typically used for superficial conditions, where low-energy photons modulate mito-

chondrial activity and inflammatory mediators without inducing significant thermal or mechanical stress.

HPLT systems deliver average powers above 1 W, often ranging from 5 to 20 W. These devices combine photochemical and photothermal effects, promoting vasodilation, extracellular matrix (ECM) remodeling, and analgesia. However, most HPLT systems lack the pulsed structure required to generate reproducible photoacoustic pressure waves.

HILT systems represent a mechanistic subset of HPLT, specifically designed to achieve a triple mechanism of action—photochemical, photothermal, and photoacoustic—through the use of high-peak power, short-duration pulses, and low duty cycles. While photochemical and photothermal mechanisms can support tissue repair across a range of laser therapies, HILT is uniquely characterized by the controlled generation of thermoelastic pressure waves that provide an additional mechanotransductive stimulus, particularly relevant for deep-tissue regeneration. These pressure waves propagate through tissues in a manner comparable to ultrasound, enabling therapeutic effects beyond the optical penetration depth of light.

To define the operational range of HILT, it is useful to refer to the classification of laser–tissue interactions proposed by Niemz [28]. This framework categorizes laser effects into five principal interaction domains based on energy density, power density, and pulse duration, as schematically illustrated in Figure 1 and described below.

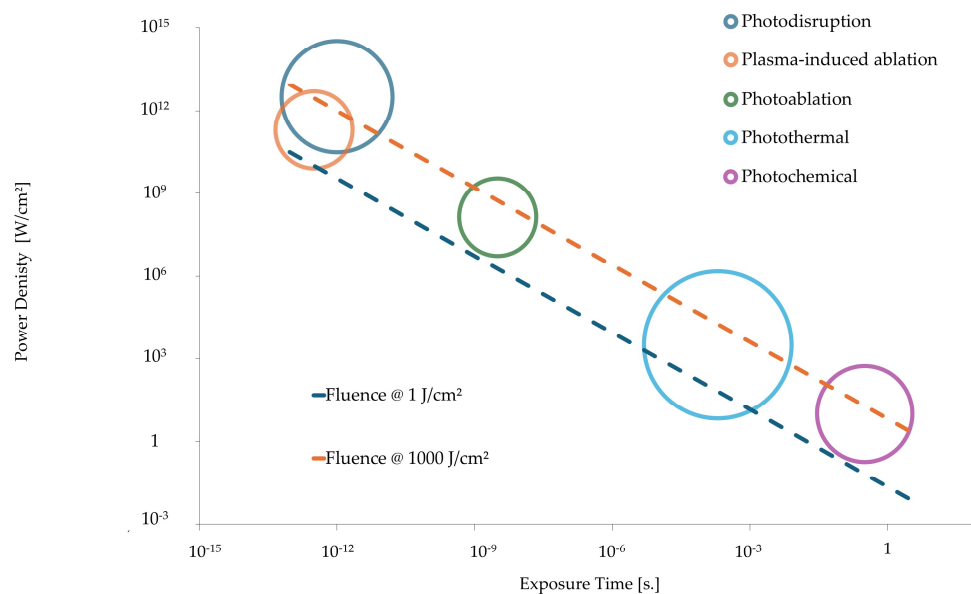


Figure 1. Map of laser–tissue interactions. Adapted from Niemz (2007) [28], who modified Boulnois (1986) [29].

Photochemical effects—Occurring at power densities below 1 W/cm² and exposure times above 10^{−3} s, these low-energy interactions primarily modulate biochemical reactions without inducing significant thermal or mechanical impact.

Photothermal effects—Observed in the range of approximately 1 W/cm² to 10⁶ W/cm², with exposure times between 10^{−6} and 10⁰ s. In this domain, absorbed optical energy is converted into heat, leading to controlled tissue warming, collagen remodeling, and vascular responses.

Photoablative effects—Typically occurring at power between 10⁶ and 10⁹ W/cm², with pulse duration in the nanosecond range. These interactions result in tissue removal through vaporization and are characteristic of precise surgical applications.

Photodisruptive effects—Associated with power densities exceeding 10⁹ W/cm² and exposure times below 10^{−9} s. In this regime, laser-induced pressure transients—

i.e., short-lived, non-stationary pressure waves generated impulsively by rapid energy deposition—lead to microcavitation and mechanical disruption.

Plasma-induced ablation—Present at extreme power densities ($>10^{12}$ W/cm²) and ultrashort pulse durations (femtosecond to nanosecond range), typically associated with ablative surgical lasers such as CO₂, Ho:YAG, and Er:YAG lasers.

The thermoelastic domain, positioned below the photoablative threshold, includes both the photochemical and photothermal interaction regimes. Within this domain, laser-induced pressure transients can be generated while avoiding irreversible tissue damage. HILT operates within this thermoelastic regime, where controlled stress waves can engage mechanotransductive pathways associated with tissue remodeling and regeneration without leading to permanent tissue disruption. To preserve this non-invasive therapeutic profile, power density is typically maintained below 10⁶ W/cm² for pulse durations in the microsecond (μs) range, thereby avoiding transitions into ablative or photodisruptive regimes. Furthermore, the in vivo energy dose (J/cm³), which quantifies the volumetric distribution of deposited energy, can be derived from the applied fluence (J/cm²) and the effective optical penetration depth (d_{eff}). At the wavelength of $\lambda = 1064$ nm, the absorption coefficient of skin in vivo is approximately $\alpha = 1.48$ cm⁻¹, about one order of magnitude higher than that of water [21]. Accordingly, the effective penetration depth can be estimated as:

$$d_{eff} = \frac{1}{\alpha} = \frac{1}{1.48} \approx 0.676 \text{ cm}$$

For an applied fluence of 1000 J/cm², the corresponding energy dose is therefore:

$$\text{Energy Dose} = \frac{1000 \text{ J/cm}^2}{0.676 \text{ cm}} \approx 1479 \text{ J/cm}^3$$

These calculations indicate that HILT operates within an in vivo energy dose of approximately 1.47 to 1479 J/cm³, depending on the applied fluence and tissue absorption properties. This range is consistent with deep-tissue stimulation while remaining within the thermoelastic regime. In contrast, surgical lasers such as CO₂, Ho:YAG (2100 nm), and Er:YAG (2940 nm) operate within the photoablation and plasma-induced ablation regimes, where both energy densities and laser-induced pressure transients far exceed thermoelastic limits. These lasers generate pressure waves exceeding millions of kPa, leading to immediate tissue fragmentation rather than controlled regenerative stimulation. The extremely high-power densities and ultrashort pulse durations characteristic of these systems promote nonlinear phenomena such as plasma formation and explosive ablation, well beyond the biophysical conditions compatible with tissue regeneration.

1.2. Theoretical Foundations of HILT-Induced Pressure Waves

The ability of HILT to induce mechanotransduction stems from the generation of pressure waves, a phenomenon governed by thermoelastic effects. Foundational studies in photoacoustics by Oraevsky et al. [30,31], along with the theoretical framework described by Wang and Wu [32] in Biomedical Optics, established the key role of pressure waves in laser-tissue interactions. Building on this foundation, Yao et al. [33] demonstrated that, for ultrashort pulses (<1 μs), pressure wave amplitude depends primarily on fluence. In contrast, in the 10–300 μs pulse range, typical of HILT, the amplitude is influenced by both fluence and laser intensity at the tissue interaction site. This dual dependence is a hallmark of HILT.

Further expanding on these principles, Esenaliev et al. [34] confirmed that pressure waves generated under thermoelastic conditions are directly proportional to laser fluence and the optical absorption coefficient of the tissue, with the Grüneisen parameter serving

as a scaling factor. This relationship is mathematically described by the thermoelastic photoacoustic pressure equation (Equation (1)):

$$P = \Gamma \mu_a F_0 \quad (1)$$

where

- P is the peak pressure (Pa),
- Γ is the Grüneisen parameter,
- μ_a is the optical absorption coefficient (cm^{-1}),
- F_0 is the laser fluence (J/cm^2).

Equation (1) highlights the direct proportionality between peak pressure and both optical absorption and fluence, with the Grüneisen parameter serving as a scaling factor.

Consistent with Equation (1), these findings reinforce that HILT remains within the thermoelastic domain, as defined by Niemz [28], where pressure waves stimulate cellular responses without exceeding the threshold for photodisruptive effects. Unlike surgical lasers (CO_2 , Ho:YAG, Er:YAG), which operate in the photodisruptive and plasma-induced ablation domains, HILT preserves tissue integrity while activating regenerative pathways.

While Equation (1) captures the fundamental thermoelastic relationship between fluence and pressure, the Margheri equation [26] (Equation (2)) provides a more precise analytical method for calculating pressure waves in laser–tissue interactions; however, its complexity limits clinical applicability. To address this limitation, we propose the Pulse Energy Dose (PED): a simplified yet effective alternative for assessing laser-induced pressure waves and ensuring that HILT systems operate safely within the thermoelastic window.

1.3. Margheri Equation for Analytical Pressure Wave Modeling

One of the key physical phenomena underlying HILT is the generation of pressure waves at the interface between air (Medium 1) and biological tissue (Medium 2). When a pulsed laser beam enters the target medium, it triggers an elastic expansion that gives rise to a pressure wave, propagating from the surface into the tissue. As illustrated in Figure 2, this transition generates an acoustic wave essential to the HILT mechanism.

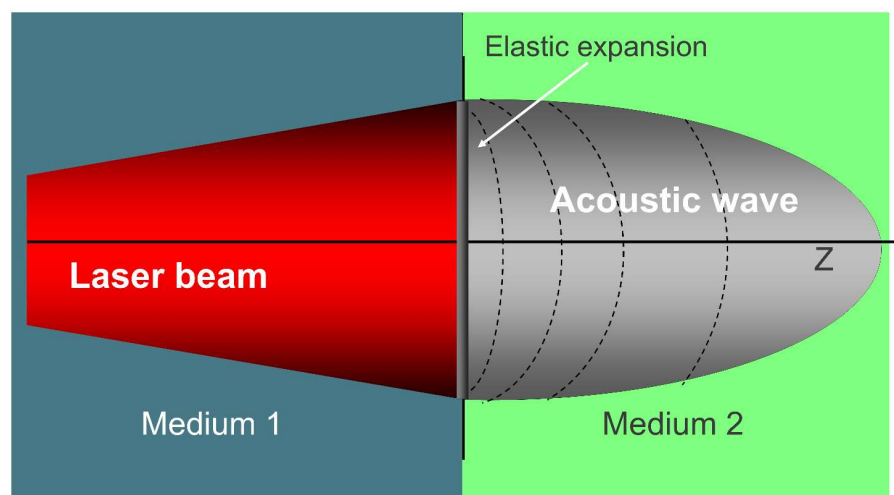


Figure 2. Photoacoustic effect: a laser beam transitions from Medium 1 to Medium 2, generating an acoustic wave through elastic expansion, key in HILT mechanisms.

The amplitude of this wave, which is critical in initiating both photoacoustic and mechanotransductive responses, depends on laser parameters and the thermophysical properties of the tissue.

The most accurate theoretical model for calculating the amplitude of laser-induced pressure waves in a biological medium is provided by Margheri [26]. The equation integrates both laser settings and tissue-specific parameters and can be expressed as Equation (2):

$$p(z, t) = f(I, v, z, t, \alpha, \rho, K, c) \quad (2)$$

where I is the peak intensity of the laser, v is the speed of sound in the medium, and the terms α (absorption coefficient), ρ (density), K (thermal conductivity), and c (specific heat) describe the intrinsic thermophysical properties of the irradiated medium.

While Equation (2) offers high theoretical accuracy, its clinical applicability is limited by the need for input parameters—such as thermal conductivity, specific heat, and tissue density—that, although well documented in biophysical literature, are rarely accessible to clinicians in real-world settings. Building on the thermoelastic dependence expressed in Equation (1), we introduce the Pulse Energy Dose (PED), a simplified yet robust metric grounded in Niemi's framework [28] and conceptually derived from the PIF model proposed by Fortuna and Masotti [27], designed to provide a more practical tool for estimating HILT-induced pressure waves in therapeutic contexts.

1.4. Biological Effects of HILT and Mechanotransduction

Mechanical pressure plays a fundamental role in cellular adaptation and tissue regeneration, not only in laser applications but also in hypergravity and mechanical loading models. Studies have shown that pressure levels in the 10–800 kPa range drive key biological processes, including cell differentiation, extracellular matrix (ECM) remodeling, and angiogenesis. These findings underscore the physiological relevance of HILT-induced pressure waves in regenerative medicine.

Monici [13], Cialdai [14], Bosco [15], Cheng [23], De Cesari [24], and Genchi [25] have demonstrated that biological responses to mechanical forces emerge at pressures as low as 10 kPa (1 G) but become significantly more pronounced at 100–800 kPa (10–80 G). This range closely aligns with the Grüneisen parameter threshold (200–800 kPa) for efficient photoacoustic stimulation in biological tissues.

For example, De Cesari et al. [24] observed that exposure to hypergravity levels of ≥ 4 G (39.2 kPa) significantly enhanced angiogenesis, cell motility, and ECM remodeling in endothelial cells. Genchi et al. [25] further showed that extreme hypergravity conditions (150 G; 1471.5 kPa) accelerate neurogenesis and neurite outgrowth, confirming the mechanosensitivity of neuronal cells.

To contextualize these findings, it is useful to convert gravitational force into pressure using the hydrostatic equation (Equation (3)):

$$p = \rho gh \quad (3)$$

where p is pressure (Pa), ρ is fluid density (kg/m^3), g is gravitational acceleration ($9.81 \text{ m}/\text{s}^2$), and h is the fluid column height (m). In water ($\rho = 1000 \text{ kg}/\text{m}^3$), 1 G corresponds to $\sim 9.81 \text{ kPa}$. As explained in The Feynman Lectures on Physics [35], pressure is a fundamental mechanical quantity that governs the behavior of matter in both static and dynamic systems.

$$p = 1000 \times 9.81 \times 1 = 9.81 \text{ kPa}$$

From Equation (3), assuming water density ($\rho \approx 1000 \text{ kg}/\text{m}^3$) and a unit column height, pressure can be directly expressed as a function of gravitational acceleration in multiples of Earth's gravity:

$$p(\text{kPa}) = G \times 9.81 \quad (4)$$

Equation (4), derived from Equation (3), allows us to express hypergravity levels in terms of pressure, making it easier to interpret their effects in various applications.

The table below (Table 1) summarizes the relationship between pressure levels and biological responses reported across different studies. In biological systems, pressure is increasingly recognized as a critical mediator of cellular responses to external mechanical forces.

1.5. HILT and HPLT: The Need for a Distinct Classification

- While High-Power Laser Therapy (HPLT) and High-Intensity Laser Therapy (HILT) are often used interchangeably in marketing and clinical contexts, this conflation is both scientifically and therapeutically misleading. Although both systems operate at average powers exceeding 1 W, their biophysical mechanisms of action depend critically on emission parameters rather than on average power alone. High-power laser configurations that are characterized by continuous or quasi-continuous emission, or by relatively high duty cycles, primarily induce photochemical and photothermal interactions. These effects include vasodilation, transient analgesia, myorelaxation, increased microcirculation, and mild tissue heating. Under such emission conditions, the generation of a reproducible thermoelastic pressure wave capable of effective deep propagation is unlikely. By contrast, when high-power laser systems are operated under parameter configurations that enable a thermoelastic photoacoustic response, they are characterized by:
 - Peak powers in the kW range,
 - Pulse durations between 10 and 300 μ s,
 - Pulse energy densities of several hundred mJ/cm² to >1 J/cm²,
 - Very low duty cycles (typically < 1%).

These configurations enable the generation of photoacoustic pressure waves that can exceed the 10–100 kPa range associated with the activation of mechanosensitive biological processes.

Table 1. Biological effects of different mechanical pressures (gravity- and laser-induced) on various target tissues.

Gravity (G)	Pressure (kPa)	Authors	Biological Effect	Target Tissue
1.1 G	10.79 kPa	Bosco et al. [22]	Neuromuscular adaptation	Leg extensor muscles
2 G	19.62 kPa	Cheng et al., [23]	Increased bone density	Bone
4 G	39.24 kPa	De Cesari et al. [24]	Pro-angiogenic activation	Endothelial cells (HMEC-1)
10 G	98.1 kPa	Monici et al. [13]	ECM remodeling and mechanotransduction	Fibroblasts, chondrocytes, endothelial cells
20 G	196.2 kPa	De Cesari et al. [24]	Vascular stimulation and coagulation regulation	Vascular endothelium
50 G	490.5 kPa	Genchi et al. [25]	Accelerated neurogenesis	PC12 neuronal cells
150 G	1471.5 kPa	Genchi et al. [25]	Enhanced neurite outgrowth and differentiation	PC12 neuronal cells
200–800 kPa	2–8 bar	Yao [33]	Pressure wave generation in laser therapy (Grüneisen parameter)	Laser-irradiated biological tissues

Abbreviations: G, gravity; kPa, kilopascal; ECM, extracellular matrix; HMEC-1, human microvascular endothelial cells. The table summarizes the relationship between pressure levels and biological responses across different studies. The pressures induced by HILT (10–800 kPa) align closely with those observed in hypergravity experiments, where mechanical stimuli promote angiogenesis, ECM remodeling, neurogenesis, and tissue regeneration.

The sharp acoustic gradients produced by such pulses are capable of engaging mechanosensitive ion channels, cytoskeletal remodeling, and fibroblast conversion—effects that are not reproducibly elicited under conventional high-duty-cycle emission conditions.

Despite this clear biophysical distinction, many high-average-power diode lasers are marketed as HILT systems, even though their emission parameters are incompatible with photoacoustic generation. This practice contributes to conceptual ambiguity and may lead to inappropriate clinical use, particularly in the treatment of deep or degenerative tissues where photoacoustic propagation is a key therapeutic component. For these reasons, a classification based on biophysical thresholds and emission parameters, rather than on average power alone, is required to guide both experimental studies and clinical protocols. The Pulse Energy Dose (PED) model introduced in this study addresses this need by providing a simplified, mechanism-specific metric for identifying photoacoustic-capable HILT configurations within the broader class of high-power laser systems.

1.6. Scope of the Study

While Equation (2) [26] provides a precise theoretical framework for calculating laser-induced pressure waves, its complexity—requiring additional biophysical parameters—limits its applicability in clinical settings. Specifically, it depends on the optical absorption coefficient, tissue density, thermal conductivity, and specific heat: values that are well known in experimental biophysics but are rarely available or considered in routine medical practice. In contrast, PED relies solely on laser usage parameters, such as peak power, frequency, and spot size, which are readily accessible to clinicians and operators.

By correlating PED-derived pressure values with biological thresholds identified in hypergravity studies, we further validate the physiological relevance of photoacoustic effects in regenerative medicine.

The specific aims of this study are to:

- Establish PED as a functional tool for classifying therapeutic laser systems, ensuring that their operating parameters fall within the thermoelastic regime, which is critical for safe therapeutic applications involving photoacoustic effects.
- Define both lower and upper operational thresholds for HILT, identifying the minimum fluence and pulse structure required to generate pressure waves above 10 kPa *in vitro*, while avoiding the transition into photoablative or photodisruptive domains, as defined by Niemz's classification [28].
- Identify the laser emission parameters and operating configurations that enable the generation of reproducible thermoelastic photoacoustic pressure waves and use these criteria to define when a high-power laser system can be operationally classified as HILT.

2. Materials and Methods

We selected a set of clinical lasers, including both surgical and therapeutic devices, operated under different parameter configurations representative of those most commonly available on the market and encountered in routine clinical practice, as described by Niemz [28] and Tunér & Hode [3]. The modeled lasers are reported in Table 2, that includes wavelength (λ), absorption coefficient (α), average and peak power, spot diameter, pulse repetition frequency (PRF), pulse duration (τ -on), and duty cycle (%).

Table 2. λ : wavelength; α : absorption coefficient; Avg Power: average output power; Peak Power: maximum instantaneous output power; Spot Diam: laser spot diameter; PRF: pulse repetition frequency; Pulse Duration τ -on: laser pulse width; Duty Cycle: ratio between pulse duration and period, expressed as percentage. T: therapeutic lasers; S: surgical lasers.

Therapeutic (T) or Surgical (S) Lasers	λ [nm]	α [cm ⁻¹]	Avg Power [W]	Peak Power [W]	Spot Diam [cm]	PRF [Hz]	Pulse Duration τ -on [μ s]	Duty Cycle [%]
S	10,600	1000.00	15	15,000.00	0.01	10	100	0.1%
S	10,600	1000.00	1.5	1500.00	0.01	10	100	0.1%
S	2940	10,000.00	15	15,000.00	0.03	10	100	0.1%
S	2940	10,000.00	2	4000.00	0.03	10	50	0.1%
S	2100	31.00	40	20,000.00	0.03	10	200	0.2%
S	2100	31.00	10	5000.00	0.03	10	200	0.2%
T	1064	0.15	2	133.33	0.5	100	150	1.5%
T	1064	0.15	2	200.00	0.5	100	100	1.0%
T	1064	0.15	1.8	300.00	0.5	60	100	0.6%
T	1064	0.15	10	1000.00	0.5	100	100	1.0%
T	1064	0.15	10	714.29	0.5	40	350	1.4%
T	1064	0.15	1.2	184.62	0.5	10	650	0.7%
T	1064	0.15	9.6	1600.00	0.5	60	100	0.6%
T	1064	0.15	10	1666.67	0.5	40	150	0.6%
T	1064	0.15	9	3000.00	0.5	30	100	0.3%
T	1064	0.15	1.2	1200.00	0.5	10	100	0.1%
T	1064	0.15	5	2500.00	0.5	20	100	0.2%
T	1064	0.15	4.5	3000.00	0.5	15	100	0.2%
T	1064	0.15	3	3000.00	0.5	10	100	0.1%
T	1064	0.15	1.5	3000.00	0.5	10	50	0.1%
T	1064	0.15	1	2000.00	0.5	5	100	0.1%
T	1064	0.15	2.1	3000.00	0.5	7	100	0.1%
T	1064	0.15	1.5	3000.00	0.5	5	100	0.1%
T	1064	0.15	20	5714.29	2	17,500	0	0.4%
T	1064	0.15	10	2857.14	1	17,500	0	0.4%
T	1064	0.15	5	1428.57	0.5	17,500	0	0.4%
T	1064	0.15	5	20.00	1	10	25,000	25.0%
T	1064	0.15	5	10.00	1	10	50,000	50.0%
T	1064	0.15	5	6.67	1	10	75,000	75.0%
T	980	0.50	20	5714.29	2	17,500	0	0.4%
T	980	0.50	10	2857.14	1	17,500	0	0.4%
T	980	0.50	5	1428.57	0.5	17,500	0	0.4%
T	980	0.50	20	80.00	3	10	25,000	25.0%
T	980	0.50	10	40.00	2	10	25,000	25.0%
T	980	0.50	5	20.00	1	10	25,000	25.0%

Table 2. Cont.

Therapeutic (T) or Surgical (S) Lasers	λ [nm]	α [cm ⁻¹]	Avg Power [W]	Peak Power [W]	Spot Diam [cm]	PRF [Hz]	Pulse Duration τ -on [μ s]	Duty Cycle [%]
T	980	0.50	5	10.00	1	10	50,000	50.0%
T	980	0.50	5	6.67	1	10	75,000	75.0%
T	910	0.08	5	20.00	1	10	25,000	25.0%
T	910	0.08	5	10.00	1	10	50,000	50.0%
T	910	0.08	5	6.67	1	10	75,000	75.0%
T	905	0.08	5	1428.57	0.5	17,500	0	0.4%
T	905	0.08	5	714.29	0.5	100,000	0	0.7%
T	810	0.02	5	20.00	1	10	25,000	25.0%
T	810	0.02	5	10.00	1	10	50,000	50.0%
T	810	0.02	5	6.67	1	10	75,000	75.0%

We modeled their behavior using Equation (2) (Margheri) and Pulse Energy Dose (PED, Equation (5)).

To accurately describe the pressure wave propagation in a biological medium, the analytical mode, developed by Margheri [26] provides a robust framework Equation (2):

$$p_2(z, t) = \rho_2 v_2^2 \cdot \frac{\alpha \sqrt{k_1 k_2}}{K_1 \sqrt{k_2} + K_2 \sqrt{k_1}} \cdot \frac{1}{v_2 + r v_1} \cdot \left(\beta_1 \sqrt{k_1} + \beta_2 \sqrt{k_2} \right) \cdot I \left(t - \frac{z}{v_2} \right)$$

where

- I is the laser pulse intensity.
- v_2 is the speed of sound in the second medium.
- z is the depth.
- t is the time of wave propagation.
- Other parameters (K_i, b_i, r_i, α) describe the medium's thermal, mechanical, and optical properties of the irradiated medium.

The Pulse Energy Dose (PED) is defined as:

$$PED = \frac{Fluence}{Penetration \times DC} \tag{5}$$

where

- $Fluence$ is the energy per pulse (E_p) divided by the spot area [cm²].
- $Penetration$ is given by $1/\alpha$, where α is the absorption coefficient of water (Palmer & Williams [36]).
- DC (Duty Cycle) is the ratio of laser pulse duration (τ -on) to the total period (T), expressed as a percentage.

In other words, we are evaluating fluence in relation to penetration depth and emission time.

Through algebraic manipulation, Equation (5) can also be expressed as:

$$PED = I_p \times \alpha \times \frac{1}{f}$$

where

- I_p is the peak power divided by the spot area.
- f is the pulse repetition frequency (Hz).

In essence, if we know the spot size, peak power, and pulse repetition frequency, we can calculate the Pulse Energy Dose (PED) in J/cm^3 .

In this model, penetration depth was assumed to be the reciprocal of the absorption coefficient, $1/\alpha$.

The goal here is to determine whether the intensity of light is capable of generating a pressure wave greater than 10 kPa and whether this wave remains within the thermoelastic regime, ensuring its suitability for therapeutic applications.

We proceeded with the calculation of both parameters: pressure wave, according to Equation (2), and Pulse Energy Dose (PED, Equation (5)). We applied the calculations to the same lasers and configurations listed in Table 3.

Table 3. Surgical Lasers, Pressure Wave [kPa] vs. PED [J/cm^3]. λ , wavelength; α , absorption coefficient; Avg Power, average power; Peak Power, peak power; Spot Diam, spot diameter; PRF, pulse repetition frequency; τ_{on} , pulse duration; Duty Cycle, ratio between pulse duration and period; PED, pulse energy.

Therapeutic (T) or Surgical (S) Lasers	λ [nm]	α [cm^{-1}]	Avg. Power [W]	Peak Power [W]	Spot Diam. [cm]	PRF [Hz]	Pulse Duration τ_{on} [μs]	Duty Cycle [%]	Pressure Wave, Margheri [kPa]	PED [J/cm^3]
S	10,600	1000.00	15	15,000.00	0.01	10	100	0.1%	6,612,218,865	19,098,593,171
S	10,600	1000.00	1.5	1500.00	0.01	10	100	0.1%	661,221,887	1,909,859,317
S	2940	10,000.00	15	15,000.00	0.03	10	100	0.1%	7,346,910,296	21,220,659,079
S	2940	10,000.00	2	4000.00	0.03	10	50	0.1%	1,959,176,079	5,658,842,421
S	2100	31.00	40	20,000.00	0.03	10	200	0.2%	30,367,163	87,712,058
S	2100	31.00	10	5000.00	0.03	10	200	0.2%	7,591,791	21,928,014

We then used statistical analysis to investigate the relationship between the pressure wave calculated using Equation (2) and Pulse Energy Dose (PED, Equation (5)). To quantify this relationship, we applied Pearson’s correlation coefficient (r), which measures the linear association between two variables. The coefficient r is expressed as Equation (6):

$$r = \frac{\sum(X_i - \bar{X})(Y_i - \bar{Y})}{\sqrt{\sum(X_i - \bar{X})^2} \sqrt{\sum(Y_i - \bar{Y})^2}} \tag{6}$$

where

- X_i represents individual pressure wave values,
- Y_i represents corresponding PED values,
- \bar{X} and \bar{Y} represent the mean values of pressure wave and PED, respectively.

A high positive correlation ($r \approx 1$) would indicate that PED can serve as a useful surrogate metric for estimating the laser-induced pressure wave.

For better visualization, results were categorized based on the type of laser: Surgical lasers, Pulsed therapeutic lasers, Superpulsed therapeutic lasers, and Chopped therapeutic lasers.

The findings are presented in a scatter plot, where the x -axis represents the pressure wave (kPa) and the y -axis represents PED (J/cm^3). This visualization allowed us to assess whether the data points followed a linear trend, further supporting the reliability of PED as a proxy for estimating laser-induced pressure waves.

We then performed a statistical analysis to investigate the relationship between the pressure wave amplitude calculated using Equation (2) and the Pulse Energy Dose (PED, Equation (5)). The strength of this relationship was quantified using Pearson's correlation coefficient (r), which measures the degree of linear association between two variables.

Correlation results were visualized using scatter plots, with pressure wave amplitude (kPa) on the x -axis and PED (J/cm^3) on the y -axis. Data points were grouped according to laser category (surgical, pulsed therapeutic, superpulsed therapeutic, and chopped therapeutic) to assess whether a consistent linear trend was observed across different laser configurations.

To evaluate the robustness of the PED model across different laser types, Pearson's correlation coefficient (r) and statistical significance ($p < 0.05$) were calculated separately for each laser category. This subgroup analysis allowed us to verify the consistency of the PED–pressure wave relationship across surgical and therapeutic laser systems.

In addition, energy dose thresholds were calculated for both *in vitro* and *in vivo* conditions to account for differences in optical absorption and laser–tissue interactions between experimental models and biological tissues. This distinction supports the application of the PED framework in both preclinical studies and clinical settings by defining appropriate operating ranges for each context.

3. Results

The study yielded three main results: (i) a strong correlation between pressure wave amplitude and PED; (ii) the identification of the minimum and maximum operational thresholds for photoacoustic effects; and (iii) the definition of laser operating conditions that enable the generation of pressure waves exceeding 10 kPa *in vitro*.

3.1. Correlation Between Pressure Wave and PED

Table 3 shows the pressure wave and energy dose values of the most used settings for soft tissue surgery. As observed, the values range from millions to billions of J/cm^3 , which, according to Niemz's [28] classification, corresponds to photoablative or plasma-induced regimes. These values are far beyond the thermoelastic regime, which is the one of interest for HILT (High-Intensity Laser Therapy).

To assess the relationship between the pressure wave calculated using Equation (2) and the Pulse Energy Dose (PED, Equation (5)), we computed Pearson's correlation coefficient (r) along with its statistical significance (see Figure 3).

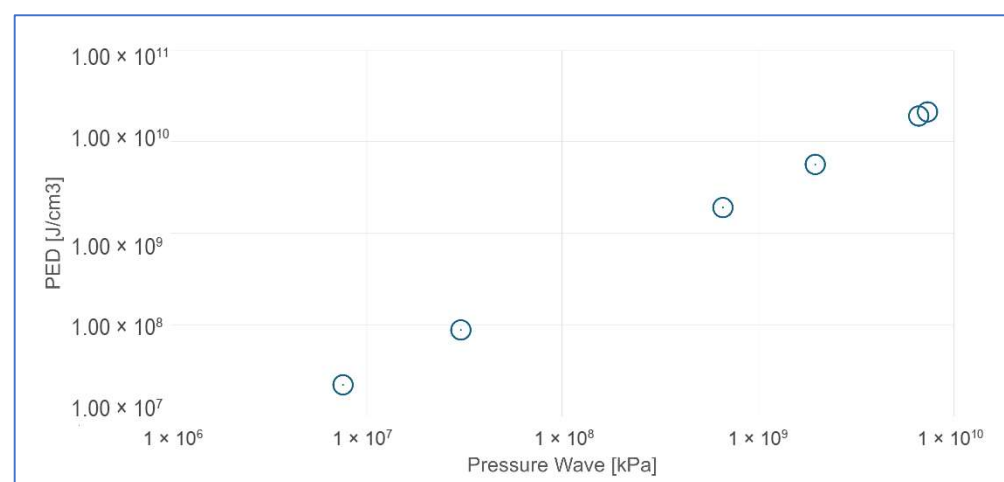


Figure 3. Scatter plot showing the relationship between Pulse Energy Dose (PED) [J/cm^3] and pressure wave amplitude [kPa] for surgical lasers (data from Table 4).

Table 4. Statistical summary of the correlation between pressure wave and pulse energy dose (PED) in surgical lasers. Abbreviations: PED, pulse energy dose; PW, pressure wave; PED/PW, ratio between PED and pressure wave; SD, standard deviation.

Surgical Lasers	Pressure Wave [kPa]	PED [J/cm ³]	PED/PW
Mean	2,769,581,014	7,999,599,010	2.888378773
Standard Deviation	3,345,194,176	9,662,187,758	2.888378746
Covariance	3.23219×10^{19}		
Pearson's r	1.00		
p-Value	9.05957×10^{-31}		

The correlation analysis between Pressure Wave [26] and PED resulted in a Pearson's correlation coefficient of $r = 1.00$, indicating an almost perfect linear relationship between the two parameters. The associated p-value ($p = 9.06 \times 10^{-31}$) confirms that this correlation is highly statistically significant, meaning that the probability of this relationship occurring by chance is virtually zero.

Table 5 shows the pressure wave and energy dose values of the most commonly used therapeutic settings in laser therapy. As observed, the values range in J/cm³, which, according to Niemi's [28] classification, corresponds to a thermoelastic regime typical of therapeutic procedures.

Table 5. Color-coded summary of therapeutic lasers, classified according to the generated pressure wave and PED values. Legend. Green rows identify real HILT devices (pressure wave > 10 kPa); pink rows indicate intermediate lasers (pressure wave between 1 and 10 kPa); white rows correspond to low-power lasers (pressure wave around 0 kPa). Abbreviations: λ, wavelength; α, absorption coefficient; Avg Power, average power; Peak Power, peak power; Spot Diam, spot diameter; PRF, pulse repetition frequency; τ-on, pulse duration; Duty Cycle, ratio between pulse duration and period; PED, pulse energy dose; PW, pressure wave.

Therapeutic (T) or Surgical (S) Lasers	λ [nm]	α [cm ⁻¹]	Avg Power [W]	Peak Power [W]	Spot Diam [cm]	PRF [Hz]	Pulse Duration τ-on [μs]	Duty Cycle [%]	Pressure Wave. Margheri [kPa]	PED [J/cm ³]
T	1064	0.148	2	133.33	0.5	100	150.00	1.50%	0.35	1.005
T	1064	0.148	2	200.00	0.5	100	100.00	1.00%	0.52	1.508
T	1064	0.148	1.8	300.00	0.5	60	100.00	0.60%	1.30	3.769
T	1064	0.148	10	1000.00	0.5	100	100.00	1.00%	2.60	7.538
T	1064	0.148	10	714.29	0.5	40	350.00	1.40%	4.65	13.460
T	1064	0.148	1.2	184.62	0.5	10	650.00	0.65%	4.82	13.916
T	1064	0.148	9.6	1600.00	0.5	60	100.00	0.60%	6.94	20.100
T	1064	0.148	10	1666.67	0.5	40	150.00	0.60%	10.85	31.407
T	1064	0.148	9	3000.00	0.5	30	100.00	0.30%	26.06	75.376
T	1064	0.148	1.2	1200.00	0.5	10	100.00	0.10%	31.30	90.451
T	1064	0.148	5	2500.00	0.5	20	100.00	0.20%	32.59	94.220
T	1064	0.148	4.5	3000.00	0.5	15	100.00	0.15%	52.16	150.752
T	1064	0.148	3	3000.00	0.5	10	100.00	0.10%	78.25	226.127
T	1064	0.148	1.5	3000.00	0.5	10	50.00	0.05%	78.25	226.127
T	1064	0.148	1	2000.00	0.5	5	100.00	0.05%	104.36	301.503
T	1064	0.148	2.1	3000.00	0.5	7	100.00	0.07%	111.81	323.039
T	1064	0.148	1.5	3000.00	0.5	5	100.00	0.05%	156.54	452.255

Table 5. Cont.

Therapeutic (T) or Surgical (S) Lasers	λ [nm]	α [cm ⁻¹]	Avg Power [W]	Peak Power [W]	Spot Diam [cm]	PRF [Hz]	Pulse Duration τ_{on} [μ s]	Duty Cycle [%]	Pressure Wave, Margheri [kPa]	PED [J/cm ³]
T	1064	0.148	20	5714.29	2	17,500	0.20	0.35%	0.00	0.015
T	1064	0.148	10	2857.14	1	17,500	0.20	0.35%	0.00	0.031
T	1064	0.148	5	1428.57	0.5	17,500	0.20	0.35%	0.00	0.062
T	980	0.502	20	5714.29	2	17,500	0.20	0.35%	0.01	0.052
T	980	0.502	10	2857.14	1	17,500	0.20	0.35%	0.03	0.104
T	980	0.502	5	1428.57	0.5	17,500	0.20	0.35%	0.06	0.209
T	905	0.075	5	1428.57	0.5	17,500	0.20	0.35%	-0.01	0.031
T	905	0.075	5	714.29	0.5	100,000	0.07	0.70%	-0.01	0.003
T	1064	0.148	5	20.00	1	10	25,000.00	25.00%	0.13	0.377
T	1064	0.148	5	10.00	1	10	50,000.00	50.00%	0.07	0.188
T	1064	0.148	5	6.67	1	10	75,000.00	75.00%	0.04	0.126
T	980	0.502	20	80.00	3	10	25,000.00	25.00%	0.20	0.568
T	980	0.502	10	40.00	2	10	25,000.00	25.00%	0.22	0.639
T	980	0.502	5	20.00	1	10	25,000.00	25.00%	0.44	1.278
T	980	0.502	5	10.00	1	10	50,000.00	50.00%	0.22	0.639
T	980	0.502	5	6.67	1	10	75,000.00	75.00%	0.15	0.426
T	910	0.075	5	20.00	1	10	25,000.00	25.00%	0.07	0.191
T	910	0.075	5	10.00	1	10	50,000.00	50.00%	0.03	0.095
T	910	0.075	5	6.67	1	10	75,000.00	75.00%	0.02	0.064
T	810	0.0191	5	20.00	1	10	25,000.00	25.00%	0.02	0.049
T	810	0.0191	5	10.00	1	10	50,000.00	50.00%	0.01	0.024
T	810	0.0191	5	6.67	1	10	75,000.00	75.00%	0.01	0.016

Table 6 shows $r \approx 0.99$, confirming a near-perfect linear relationship between Pressure Wave and PED that remains, extremely strong. The constant PED/PW ratio (~ 2.89) indicates that PED can reliably predict the pressure wave across different therapeutic laser configurations. The p -value is close to zero, ensuring that this correlation is highly statistically significant and not due to random variation.

Table 6. Statistical summary of the correlation between pressure wave and pulse energy dose (PED) in therapeutic lasers. Abbreviations: PED, pulse energy dose; PW, pressure wave; PED/PW, ratio between PED and pressure wave; SD, standard deviation; Pearson’s r , correlation coefficient.

Therapeutic Lasers	Pressure Wave [kPa]	PED [J/cm ³]	PED/PW
Mean	18	52	2.89
Standard Deviation	37	108	2.89
Covariance	4034.109101		
Pearson’s r	0.999999975		
p -Value	8.9669×10^{-137}		

The absolute values of both Pressure Wave and PED are significantly lower, meaning that the system is within a thermoelastic regime, which is desirable for HILT applications.

The Scatter Plot illustrates the relationship between Pressure Wave [26] and PED for therapeutic lasers (see Figure 4).

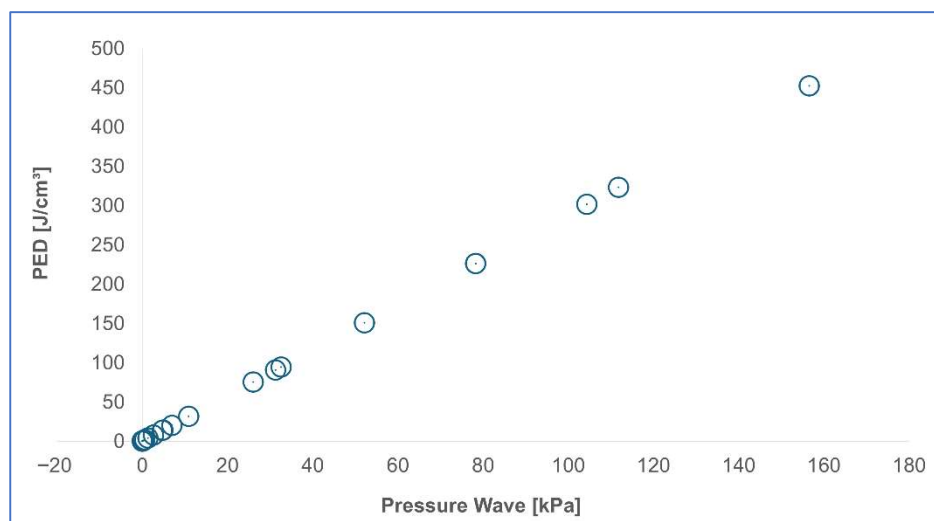


Figure 4. Scatter plot showing the relationship between Pulse Energy Dose (PED) [J/cm³] and Pressure Wave [kPa] for therapeutic lasers.

3.2. Thresholds (MIN and MAX) for Photoacoustic Effects

Our results indicate that a minimum Energy Dose (ED) of 30 J/cm³ is required to generate a pressure wave exceeding 10 kPa, a threshold identified as sufficient for inducing reproducible photoacoustic effects. This threshold, represented by the green band (Table 6), marks the baseline for effective photoacoustic interaction.

To translate fluence (*F*) into Energy Dose (*ED*), we applied the formula:

$$ED = F \times \frac{1}{\alpha}$$

where the depth of penetration is approximated as the reciprocal of the absorption coefficient $1/\alpha$ for each wavelength (λ). This conversion allowed us to construct Table 7, which establishes the upper and lower energy dose limits for different laser wavelengths in vitro and in vivo. Accordingly, the identified ED thresholds can be consistently interpreted within the Pulse Energy Dose framework defined in Equation (5).

Table 7. Maximum pulse energy dose (PED) limits in vitro and in vivo for different laser wavelengths. Abbreviations: λ , wavelength; α , absorption coefficient; $1/\alpha$, optical penetration depth; Max ED, maximum energy dose; PED, pulse energy dose. Note: Reported values indicate threshold PED levels associated with tissue optical properties, distinguishing between in vitro and in vivo experimental conditions.

λ [nm]	α [cm ⁻¹]	$1/\alpha$ [cm ⁻¹]	Max ED [J/cm ³] Vitro	Max ED [J/cm ³] Vivo
10,600	1000.00	0.0010	1,000,000	10,000,000
2940	10,000.00	0.0001	10,000,000	100,000,000
2100	31.00	0.0323	31,000	310,000
1064	0.15	6.7568	148	1480
980	0.50	1.9920	502	5020
910	0.08	13.3333	75	750
905	0.06	16.4204	61	609
810	0.02	52.3560	19	191

Nd: YAG (1064 nm): the maximum *ED* in vivo is approximately 1480 J/cm³. Exceeding this value may lead to overstimulation.

Diode lasers (980–810 nm): the upper limit ranges from 5020 J/cm³ (980 nm) to 191 J/cm³ (810 nm).

Highly absorbent wavelengths (Er: YAG—2940 nm, CO₂—10,600 nm): these lasers exhibit exceptionally high ED values, exceeding practical therapeutic applications.

3.3. Comparison of High-Power Laser Configurations Based on Photoacoustic Capability

The analysis of the data reported in Table 5 (color-coded table) indicates that, within the broad category of high-power laser systems, three distinct parameter configurations emerge, characterized by different abilities to generate thermoelastic pressure waves. Rather than defining rigid therapeutic categories, this classification reflects clusters of laser operating conditions that occupy different regions with respect to the photoacoustic threshold.

Green zone (photoacoustic-capable configurations).

This region includes laser configurations that generate pressure waves in the range of approximately 10–150 kPa under the tested in vitro conditions. These parameter sets—characterized by kilowatt-range peak power, microsecond pulse duration, high pulse energy, and very low duty cycle—correspond to operating conditions capable of reliably inducing a thermoelastic photoacoustic effect. Laser systems operated within this region can therefore be described as functioning according to what is commonly referred to as High-Intensity Laser Therapy (HILT).

Pink zone (near-threshold configurations).

The intermediate region includes laser configurations that do not exceed the 10 kPa threshold in vitro but approach it closely. Given the substantially higher optical absorption coefficients of biological tissues compared with water, these configurations may exceed the photoacoustic threshold in vivo, depending on wavelength and tissue properties. This zone represents a transitional regime in which small changes in laser parameters or tissue absorption may determine whether a measurable photoacoustic contribution is present.

White zone (non-photoacoustic configurations).

The white region comprises high-power laser configurations that remain well below the photoacoustic threshold under all tested conditions. These include pulsed, super-pulsed, and chopped systems operating at various wavelengths and spot sizes, whose parameter combinations do not allow the generation of thermoelastic pressure waves, even under optimized settings. Such configurations remain dominated by photochemical and photothermal interactions.

Importantly, this analysis does not propose a dichotomous opposition between HILT and HPLT. Instead, it demonstrates that HILT represents a specific subset of high-power laser therapy, defined by the emergence of a reproducible photoacoustic component when particular combinations of peak power, pulse duration, pulse energy, and repetition rate are employed.

A quantitative comparison further highlights the separation between photoacoustic-capable and non-photoacoustic configurations:

- Minimum Energy Dose associated with photoacoustic-capable configurations: 31.41 J/cm³;
- Maximum Energy Dose observed in non-photoacoustic configurations: 1.28 J/cm³;
- Relative difference (Δ): +2457%;
- Separation between regimes: 1.39 orders of magnitude (log₁₀ scale).

These results support the concept that the ability to generate thermoelastic pressure waves is not an intrinsic property of laser power alone but rather emerges from specific parameter configurations within the broader class of high-power laser systems.

4. Discussion

The findings of this study confirm that Pulse Energy Dose (PED, Equation (5)) is a reliable and accessible tool for assessing a laser system's ability to generate meaningful photoacoustic effects. We propose PED as a simplified yet clinically practical alternative to Equation (2) [26], which—although more precise in directly calculating photoacoustic pressure—is often too complex for routine clinical application. For practical and clinical use, Equation (5) can be expressed in an operational form that relies exclusively on parameters that are either directly available on laser devices or commonly known in clinical practice:

$$PED = \frac{I_p \cdot \alpha}{f}$$

where I_p represents peak intensity [W/cm^2], α is the absorption coefficient [cm^{-1}], and f is the pulse repetition frequency [Hz]. This operational formulation makes PED particularly suitable for clinical use, as it depends on parameters that clinicians can directly set or readily retrieve, enabling a rapid and informed assessment of a laser system's photoacoustic potential.

It is important to note that the Pulse Energy Dose formulation is not specific to a single wavelength, as wavelength dependence is inherently accounted for through the absorption coefficient α , which is characteristic of each tissue–wavelength combination.

The proposed pressure threshold should not be interpreted as a necessary condition for biological response but rather as a sufficient condition to ensure the emergence of a robust and reproducible photoacoustic component under thermoelastic conditions.

It should be clarified that the binary distinction between low-level laser therapy (LLLT) and higher-power laser systems was not introduced in this study but is well established in the existing laser therapy nomenclature. The present work does not propose a new dichotomy based on therapeutic efficacy. Rather, it addresses the internal heterogeneity of high-power laser systems by demonstrating that, above the conventional LLLT range, only a specific subset of lasers operated under defined pulsed conditions can generate thermoelastic pressure waves. These systems are therefore identified as a distinct subcategory—High-Intensity Laser Therapy (HILT)—within the broader class of high-power laser therapy (HPLT). This classification is based on the emergence of a photoacoustic mechanism, not on a presumed superiority of clinical outcomes, and explicitly acknowledges that other high-power systems may still produce meaningful photochemical and photothermal effects without generating pressure waves.

Below this threshold, photobiomodulation may still yield excellent therapeutic outcomes, but these effects are driven by photochemical rather than by photoacoustic processes. The present framework does not question the efficacy of PBM or of photothermal treatments but specifically delineates the conditions under which photoacoustic stimulation becomes a distinct and dominant physical mechanism. Although higher average power is commonly assumed to correlate with improved therapeutic outcomes, our results show that not all High-Power Laser Therapy (HPLT) devices can produce effective pressure waves, even when their nominal specifications appear similar. The analysis of various systems underscores that peak power and pulse structure, not average power, are the key determinants in defining a photoacoustic-capable HILT configuration.

For example, a 1064 nm pulsed laser operating at an average power of only 1.5 W but delivering a peak power of 3000 W with a pulse duration of 100 μs and a repetition rate of 5 Hz can generate pressure waves of approximately 150 kPa in water. Considering that the optical absorption coefficient of skin is approximately one order of magnitude higher than that of water, this corresponds to estimated *in vivo* pressure levels on the order of 1500 kPa, as reported by Salomatina et al. [21]. In contrast, a 10 W pulsed 1064 nm laser with identical

spot size (5 mm), but operating at 100 Hz and with a lower peak power of 1000 W, generates only 7.5 kPa in water, well below the threshold needed for photoacoustic stimulation.

This comparison underscores a crucial aspect of HILT classification: power alone does not determine whether a laser is likely to deliver a meaningful photoacoustic component under thermoelastic conditions. Instead, the relationship between peak power, pulse duration, and repetition frequency dictates whether a system can truly qualify as High-Intensity Laser Therapy or if it remains in the category of High-Power Lasers without significant photoacoustic effects.

At this stage, it is important to emphasize that the lack of clear mechanistic classification has historically contributed to heterogeneous and sometimes difficult-to-interpret results in the laser therapy literature. In studies labeled as HPLT, transient photoacoustic components may occasionally be present but remain unrecognized or uncontrolled, while conversely, a substantial portion of the literature referring to HILT includes laser systems that, despite their nomenclature, do not generate measurable photoacoustic pressure waves. This overlap does not invalidate prior findings but highlights the need for objective physical criteria to distinguish photothermal, photochemical, and photoacoustic contributions. The framework proposed in this study is specifically intended to reduce this ambiguity by providing a transparent and reproducible method to identify when thermoelastic pressure waves are reliably generated, thereby improving the interpretability and comparability of both HPLT and HILT studies.

The generation of an acoustic pressure wave is not merely a technical parameter but has fundamental biological relevance. From a cellular perspective, the mechanotransductive effects discussed in this study are not hypothetical but are grounded in well-established molecular mechanisms extensively described in the literature on mechanical stimulation and hypergravity. Mechanical forces in the range considered here are known to activate mechanosensitive ion channels, including stretch-activated calcium channels, Piezo channels, and TRP family channels, leading to transient increases in intracellular Ca^{2+} . These signals are transmitted through the cytoskeleton via integrins and focal adhesion complexes, activating downstream pathways such as MAPK/ERK and other mechanoresponsive signaling cascades that regulate gene expression, differentiation, and extracellular matrix remodeling. Notably, the present study does not aim to identify novel molecular pathways but rather to define the physical conditions under which these well-known mechanotransductive mechanisms can be reliably engaged by laser-induced thermoelastic pressure waves.

One of the primary reasons for inducing a pressure wave is to replicate the beneficial effects observed in regenerative medicine through hypergravity models [13,14,22–25], where mechanical stimuli have been shown to enhance cell differentiation, extracellular matrix remodeling, and tissue regeneration. Studies on hypergravity have demonstrated that pressures ranging from 10 kPa [22] to 800 kPa [33] significantly influence cellular behavior, angiogenesis, and osteogenesis, reinforcing the idea that mechanotransduction is a key driver of regenerative processes. In this context, HILT acts as a non-invasive alternative to mechanical stimulation, delivering energy in a way that mimics the effects of hypergravity at the cellular level. It is also important to emphasize that the cellular stimulation protocols used in hypergravity studies are typically acute and time-limited, with exposure durations ranging from a few minutes to tens of minutes, rather than chronic or sustained loading. This temporal profile closely mirrors the duration of a standard HILT treatment session, which is likewise delivered over minutes through a sequence of transient mechanical stimuli. Therefore, the mechanotransductive responses described in hypergravity models are directly comparable, in terms of exposure time and stimulus nature, to those induced by HILT-generated thermoelastic pressure waves. Importantly, the

mechanotransductive framework discussed here refers to acute, time-limited mechanical stimulation, comparable in duration to standard HILT treatment sessions, rather than to chronic loading conditions.

Beyond its role in mechanotransduction, the ability of HILT to generate pressure waves carries additional biological significance. Unlike light, which is rapidly absorbed and scattered within the first few millimeters of tissue, the thermoelastic pressure waves generated by HILT exhibit characteristic frequency components in the kilohertz range and can therefore penetrate several centimeters into biological tissues, experiencing substantially lower attenuation than conventional megahertz ultrasound, particularly in heterogeneous soft tissues. From a biological perspective, it is important to distinguish between effects mediated by light and those mediated by pressure waves. Low-level lasers primarily induce photochemical and photothermal responses in superficial tissues, improving microcirculation, neural modulation, and cellular metabolism, but remain constrained by the physical limits of light penetration. In contrast, the thermoelastic pressure waves generated by HILT propagate into deeper tissues and stimulate cellular responses through mechanotransductive pathways. In this context, low-level laser stimulation does not overlap with photoacoustic stimulation but rather improves the biological boundary conditions under which deep mechanical stimulation can be most effectively expressed.

Another critical aspect of HILT-induced pressure waves is their temporal sequence in tissue interaction. Light energy is deposited first, rapidly giving rise to a pressure wave through thermoelastic expansion, while thermal diffusion develops on a longer timescale. This chronological order is fundamental because each of these energy forms contributes distinct biological effects. Photochemical effects, as previously described in the introduction, trigger metabolic and biochemical responses through Cytochrome C oxidase activation, leading to increased ATP production and reactive oxygen species (ROS) modulation [2,4]. Photothermal effects, which dominate in HPLT systems, induce controlled heating that can enhance vascularization and collagen remodeling. However, as shown by Cronshaw et al. [6] when not properly regulated, elevated tissue temperatures may lead to protein denaturation, mitochondrial dysfunction, and metabolic stress, underscoring the importance of precise dose and beam control in therapeutic applications. Moreover, recent experimental findings support this need for dosage control. In a 2025 *in vitro* study, Sleep et al. [4] demonstrated in MG-63 osteoblasts that continuous-wave photobiomodulation using multi-wavelength LEDs (700, 850, and 980 nm) significantly enhanced mitochondrial respiration and osteogenic gene expression at moderate doses (5.3 J/cm²). Taken together, these considerations highlight that photothermal stimulation remains biologically beneficial only within well-controlled exposure conditions, a principle that is consistent with clinical dermatological observations [37] showing that cumulative local heat exposure, even below burn threshold, can lead to cutaneous alterations. This clinical awareness is reflected in the prudential strategies adopted in high-power laser practice to limit sustained local heating during repeated or high-duty-cycle exposures. In high-power laser therapy, safety at elevated duty cycles is commonly ensured by increasing the spot size of the handpiece, thereby distributing energy over a larger tissue area. At high duty cycles, this geometric strategy is often necessary to prevent excessive thermal accumulation, since limited off-times restrict heat dissipation between pulses. While this approach effectively reduces local thermal load and allows treatment of broader regions, it also leads to a quadratic reduction in power density and peak intensity, since these parameters scale inversely with the square of the spot diameter. As a direct consequence, enlarging the spot size progressively shifts high-power laser configurations away from the photoacoustic regime, unless average power is increased proportionally. For example, doubling the spot diameter requires approximately a fourfold increase in average power to

preserve the same peak intensity conditions. This geometrical constraint highlights why many clinically safe high-power laser systems, despite operating at elevated average powers, remain intrinsically incapable of generating reproducible thermoelastic pressure waves and instead act predominantly through photochemical and photothermal mechanisms. These findings suggest that photoacoustic-capable HILT configurations uniquely add a mechanical stimulation component that complements photochemical and photothermal effects, thereby extending the range of biological responses achievable within high-power laser therapy. This synergy between photochemical, photothermal, and photoacoustic interactions explains why photoacoustic-capable HILT configurations represent a distinct mechanistic subset within high-power laser therapy, rather than a simple extension of conventional photothermal or photobiomodulation-based approaches.

The concept of thermoelasticity, first defined by Niemz [28], further reinforces the distinct nature of HILT. A photoacoustic-capable HILT configuration operates strictly within the thermoelastic regime, where the energy delivered is sufficient to generate a pressure wave but does not reach the threshold for photodisruptive or ablative effects. If a laser exceeds the thermoelastic limit, it transitions into the photodisruptive domain, characterized by excessive pressure waves that can fragment tissue rather than stimulate regenerative responses. This study confirms that HILT remains within the safe and effective thermoelastic range, ensuring that mechanical stimulation occurs without causing structural damage.

A crucial factor in maintaining this balance is the τ -off period, or the resting time between laser pulses. Because thermal energy dissipates slowly, excessive repetition rates risk accumulating heat and shifting the system from thermoelasticity to a purely photothermal mode. HILT systems mitigate this by employing low repetition frequencies (5–30 Hz), particularly when high-energy pulses are used. This controlled pulse structuring ensures that the desired photoacoustic effects occur while preventing thermal damage.

The results of this study also demonstrate a strong correlation between Pulse Energy Dose (PED, Equation (5)) and the pressure wave amplitude calculated using Equation (2) [26], confirming that PED is a reliable surrogate for determining a laser's ability to generate effective photoacoustic stimulation.

This was quantitatively confirmed in our correlation analysis (Table 5), where the relationship between PED and pressure wave amplitude showed a statistically significant correlation ($p < 0.0001$). This supports the proportionality between the two parameters, with a conversion factor of approximately 2.888 across different surgical laser settings.

A similar result was obtained for therapeutic lasers (Table 7), confirming that PED can reliably predict pressure wave amplitude in both clinical and experimental contexts.

Although Equation (2) provides a precise estimation of photoacoustic pressure waves, its complexity limits clinical usability. Pulse Energy Dose (PED, Equation (5)) simplifies this evaluation, making it accessible to clinicians and operators who require a straightforward method to determine whether a laser system qualifies as a photoacoustic-capable HILT configuration.

Beyond theoretical validation, clinical cases further reinforce the significance of HILT in regenerative applications. Temporomandibular joint (TMJ) therapy, for instance, has demonstrated significant improvement in pain reduction and joint function when treated with photoacoustic-capable HILT configurations, with pressure wave levels exceeding 50 kPa. Similarly, bone healing in post-extraction sites and surgical palatal expansion cases reveals accelerated osteogenesis and improved tissue regeneration, likely due to the combination of photochemical, photothermal, and photoacoustic effects. Importantly, the pressure wave values calculated in vitro are consistently lower than those expected in vivo, as biological tissues have significantly higher absorption coefficients than water [21], leading to even greater mechanical stimulation under clinical conditions.

These findings highlight the necessity of establishing precise classification criteria for HILT.

Moreover, these findings are consistent across both surgical and therapeutic laser categories. As shown in Table 7, PED proves to be an excellent predictor of pressure wave amplitude even for therapeutic lasers, further supporting its clinical relevance as a universal evaluation metric.

This predictive capacity is particularly significant when evaluating thresholds for photoacoustic stimulation. In vitro, where water is the predominant absorber, a minimum pressure wave amplitude of 10 kPa is typically required to trigger mechanotransduction. However, in vivo, due to the significantly higher absorption coefficients of biological tissues, sometimes up to an order of magnitude greater, as reported by Salomatina et al. [21], even devices that fall within the pink zone of the reference tables can exceed this 10 kPa threshold. Conversely, lasers classified in the white zone appear insufficient to generate such pressure waves, even under in vivo conditions, and should therefore be more accurately categorized as High-Power Laser Therapy (HPLT) systems, not HILT.

To determine the upper boundary of safe photoacoustic stimulation, we referenced Niemz's classification [28] of the thermoelastic regime, defined by energy fluence values ranging from 1 J/cm² to 1000 J/cm². Since our analysis emphasizes biological safety rather than technological limits, this range was adopted as the operational framework for identifying safe and effective HILT use.

These results enable a clear distinction between different operating regimes within high-power laser systems. Despite variations in emission modes (pulsed, superpulsed, or chopped), configurations located in the white zone of Table 5 remain well below the 10 kPa photoacoustic threshold and do not generate reproducible thermoelastic pressure waves under the tested conditions. The observed 1.39 orders-of-magnitude gap between configurations located in the green zone and those in the white zone of Table 5 highlights a clear separation in operating regimes. Configurations in the white zone remain far from the photoacoustic threshold and cannot be considered photoacoustic-capable HILT configurations, as they fail to generate reproducible thermoelastic pressure waves.

Based on the results of this study, laser configurations falling within the green zone must meet the following requirements:

- PED > 30 J/cm³ in vitro (or > 3.7 J/cm³ in vivo)
- Pressure wave amplitude > 10 kPa
- Peak power in the kW range
- Optimized pulse structure with controlled τ_{on} and τ_{off}

This classification ensures that only lasers capable of generating significant photoacoustic effects are labeled as HILT, preventing the widespread misclassification of high-power lasers that lack true regenerative capabilities.

5. Conclusions

This study establishes a clear and objective framework for classifying High-Intensity Laser Therapy (HILT) systems by introducing Pulse Energy Dose (PED) as a practical and clinically relevant tool. The findings demonstrate that PED correlates strongly with a laser's ability to generate photoacoustic effects, offering a simplified yet accurate metric for identifying laser configurations capable of operating within the thermoelastic regime, under which reproducible photoacoustic stimulation can occur. It should be emphasized that this framework does not challenge the well-established efficacy of photobiomodulation; rather, it delineates the physical conditions under which photoacoustic stimulation emerges as an additional and independent mechanism, complementing photochemical and photothermal effects. As wavelength dependence is intrinsically embedded in the absorption coefficient,

PED can be consistently applied across different laser wavelengths, supporting its use as a general and clinically relevant evaluation metric rather than a wavelength-specific model.

Importantly, the proposed framework refines the classification of high-power laser systems by identifying HILT as a specific mechanistic subset within HPLT, rather than introducing a new binary therapeutic categorization.

The study accomplishes three key objectives. Firstly, it validates PED as a reliable tool for distinguishing photoacoustic-capable HILT configurations from conventional High-Power Laser Therapy (HPLT) devices, demonstrating that only lasers with $\text{PED} > 30 \text{ J/cm}^3$ in vitro (or $>3.7 \text{ J/cm}^3$ in vivo) consistently generate pressure waves exceeding 10 kPa, a threshold identified as sufficient to engage mechanotransductive responses under the investigated conditions. Secondly, it defines the operational boundaries within which HILT systems remain within the thermoelastic regime, ensuring that these lasers remain within the thermoelastic window and avoid transitioning into ablative or disruptive regimes, in accordance with Niemz's classification [28] of laser–tissue interactions. Thirdly, it compares high-power laser systems on the basis of objective physical parameters, emphasizing the role of peak power, pulse structure, and duty cycle in determining photoacoustic performance.

From a clinical perspective, these findings support a more informed evaluation of high-power laser systems by emphasizing the relevance of PED values and pressure wave generation as objective physical parameters. The case studies presented further support to this distinction, illustrating the potential clinical relevance of photoacoustic-capable HILT configurations in regenerative applications, including bone healing, soft tissue repair, and joint therapy.

Future research should focus on refining treatment protocols for different tissue types, optimizing pulse structures for enhanced photoacoustic stimulation, and exploring long-term cellular and extracellular responses to HILT. Furthermore, the standardization of PED metrics and pressure wave classifications will be essential to ensure consistency across clinical applications and improve the overall efficacy of HILT-based therapies.

In conclusion, PED emerges as a critical parameter for identifying photoacoustic-capable HILT configurations. By defining both biophysical and biological thresholds for effective operation, this study lays the groundwork for a more objective and mechanism-based classification of high-power laser systems in therapeutic and regenerative contexts.

Author Contributions: Conceptualization, D.F. and F.R.; Methodology, D.F.; Investigation, D.F.; Data Curation, D.F.; Writing—Original Draft Preparation, D.F.; Writing—Review and Editing, D.F., F.M., S.P. and F.R.; Visualization, D.F.; Supervision, F.R. All authors have read and agreed to the published version of the manuscript.

Funding: This research received no external funding.

Institutional Review Board Statement: Not applicable.

Informed Consent Statement: Not applicable.

Data Availability Statement: The original contributions presented in this study are included in the article.

Acknowledgments: The authors thank El.En. S.p.A. (Florence, Italy), DEKA Dental Lasers (Tampa, FL, USA), and the Institute of Applied Physics (CNR-IFAC, Florence, Italy) for scientific discussions and support.

Conflicts of Interest: Fabrizio Margheri is employed in the R&D department of El.En. Group (Florence, Italy), which is one of several manufacturers of HILT devices worldwide. Scott Parker is employed as VP of Clinical Affairs at DEKA Dental Lasers (Nashville, TN, USA), which is among several companies marketing HILT devices in dentistry. Damiano Fortuna serves as an external

consultant for DEKA Dental Lasers (Nashville, TN, USA). The authors declare that these affiliations did not influence the design, analysis, or interpretation of the present review.

References

- Mester, A.; Mester, A. The History of Photobiomodulation: Endre Mester (1903–1984). *Photomed. Laser Surg.* **2017**, *35*, 393–394. [[CrossRef](#)] [[PubMed](#)]
- Karu, T. Photobiology of low-power laser effects. *Health Phys.* **1989**, *56*, 691–704. [[CrossRef](#)] [[PubMed](#)]
- Tunér, J.; Hode, L. *The Laser Therapy Handbook: A Guide for Research Scientists, Doctors, Dentists, Veterinarians and Other Interested Parties Within the Medical Field*; Prima Books: Grängesberg, Sweden, 2004.
- Sleep, S.; Hryciw, D.H.; Walsh, L.J.; Ranjit, E.; Tomy, N.; Arany, P.R.; George, R. Effects of Multiple Near-Infrared LEDs (700, 850, and 980 nm) CW-PBM on Mitochondrial Respiration and Gene Expression in MG63 Osteoblasts. *J. Biophotonics* **2025**, *18*, e70015. [[CrossRef](#)]
- Lawrence, J.; Sorra, K. Photobiomodulation as Medicine: Low-Level Laser Therapy (LLLT) for Acute Tissue Injury or Sport Performance Recovery. *J. Funct. Morphol. Kinesiol.* **2024**, *9*, 181. [[CrossRef](#)] [[PubMed](#)]
- Cronshaw, M.; Parker, S.; Grootveld, M.; Lynch, E. Photothermal Effects of High-Energy Photobiomodulation Therapies: An In Vitro Investigation. *Biomedicines* **2023**, *11*, 1634. [[CrossRef](#)]
- Zhang, Z.; Zhang, Z.; Liu, P.; Xue, X.; Zhang, C.; Peng, L.; Shen, W.; Yang, S.; Wang, F. The Role of Photobiomodulation to Modulate Ion Channels in the Nervous System: A Systematic Review. *Cell. Mol. Neurobiol.* **2024**, *44*, 79. [[CrossRef](#)]
- Orchardson, R.; Peacock, J.M.; Whitters, C.J. Effect of pulsed Nd:YAG laser radiation on action potential conduction in isolated mammalian spinal nerves. *Lasers Surg. Med.* **1997**, *21*, 142–148. [[CrossRef](#)]
- Alayat, M.S.; Battecha, K.H.; Elsodany, A.M.; Ali, M.I. Pulsed Nd:YAG laser combined with progressive pressure release in the treatment of cervical myofascial pain syndrome: A randomized control trial. *J. Phys. Ther. Sci.* **2020**, *32*, 422–427. [[CrossRef](#)]
- Mikhaylov, V.A. Laser Therapy in the Complex Prevention and Treatment of COVID-19 (Preliminary Results). *Int. J. Clin. Case Rep. Rev.* **2021**, *6*, 2. [[CrossRef](#)]
- Alghitany, A.; Khalil, M.; Eladl, A.; Gad, A.; Elgendy, A. The Effect of Laser Acupuncture on Immunomodulation and Dyspnea in Post-COVID-19 Patients. *Adv. Rehabil.* **2023**, *37*, 34–43. [[CrossRef](#)]
- Tarantino, C.; Rossi, G.; Flamini, G.; Fortuna, D. Cytoproliferative activity of the HILT: In vitro survey. *Lasers Med. Sci.* **2002**, *17*, A22.
- Monici, M.; Cialdai, F.; Fusi, F.; Romano, G.; Pratesi, R. Effects of pulsed Nd:YAG laser at molecular and cellular level—A study on the basis of Hilterapia[®]. *Energy Health* **2009**, *3*, 26–33.
- Cialdai, F.; Monici, M. Relationship between cellular and systemic effects of pulsed Nd:YAG laser. *Energy Health* **2010**, *5*, 4–9.
- Bucala, R.; Spiegel, L.A.; Chesney, J.; Hogan, M.; Cerami, A. Circulating fibrocytes define a new leukocyte subpopulation that mediates tissue repair. *Mol. Med.* **1994**, *1*, 71–81. [[CrossRef](#)] [[PubMed](#)]
- Andersson-Sjöland, A.; Nihlberg, K.; Eriksson, L.; Bjermer, L.; Westergren-Thorsson, G. Fibrocytes and the tissue niche in lung repair. *Respir. Res.* **2011**, *12*, 76. [[CrossRef](#)]
- Fortuna, D.; Rossi, G.; Zati, A.; Cardillo, I.; Bilotta, T.W.; Pinna, S.; Venturini, A.; Masotti, L. Nd:YAG laser in experimentally induced chronic degenerative osteoarthritis in heavyline chicken broiler—Pilot study. *Proc. SPIE* **2002**, *4903*, 77–84.
- Fortuna, D.; Rossi, G.; Zati, A.; Gazzotti, V.; Bilotta, T.W.; Pinna, S.; Venturini, A.; Masotti, L. High Intensity Laser Therapy in experimentally induced chronic degenerative tenosynovitis in heavyline chicken broiler. *Proc. SPIE* **2002**, *4903*, 85–91.
- Fortuna, D.; Rossi, G.; Paolini, C.; Magi, A.; Losani, F.; Fallaci, S.; Pacini, F.; Porciani, C.; Sandler, A.; Dalla Torre, R.; et al. The Nd:YAG pulsed wave laser as support therapy in the treatment of teno-desmopathies of athlete horses: A clinical and an experimental trial. *Proc. SPIE* **2002**, *4903*, 105–118.
- Zati, A.; Desando, G.; Cavallo, C.; Buda, R.; Giannini, S.; Fortuna, D.; Facchini, A.; Grigolo, B. Treatment of human cartilage defects by means of Nd:YAG Laser Therapy. *J. Biol. Regul. Homeost. Agents* **2012**, *26*, 701–711.
- Salomatina, E.; Jiang, B.; Novak, J.; Yaroslavsky, A.N. Optical properties of normal and cancerous human skin in the visible and near-infrared spectral range. *J. Biomed. Opt.* **2006**, *11*, 064026. [[CrossRef](#)]
- Bosco, C. Adaptive response of human skeletal muscle to simulated hypergravity condition. *Acta Physiol. Scand.* **1985**, *124*, 507–513. [[CrossRef](#)]
- Cheng, G.; Yu, B.; Song, C.; Zablotskii, V.; Zhang, X. Bioeffects of Microgravity and Hypergravity on Animals. *Chin. J. Electr. Eng.* **2023**, *9*, 29–46. [[CrossRef](#)]
- De Cesari, C.; Barravecchia, I.; Pyankova, O.V.; Vezza, M.; Germani, M.M.; Scebbba, F.; van Loon, J.J.W.A.; Angeloni, D. Hypergravity Activates a Pro-Angiogenic Homeostatic Response by Human Capillary Endothelial Cells. *Int. J. Mol. Sci.* **2020**, *21*, 2354. [[CrossRef](#)]
- Genchi, G.G.; Cialdai, F.; Monici, M.; Mazzolai, B.; Mattoli, V.; Ciofani, G. Hypergravity stimulation enhances PC12 neuron-like cell differentiation. *Biomed. Res. Int.* **2015**, *2015*, 748121. [[CrossRef](#)] [[PubMed](#)]

26. Margheri, F. Sviluppo di Trasduttori Acusto-Ottici Miniaturizzati per Diagnostica Clinica e Controlli non Distruttivi. Ph.D. Thesis, Università degli Studi di Firenze, Firenze, Italy, 2000.
27. Fortuna, D.; Masotti, L. The HILT domain by the pulse intensity fluence (PIF) formula. *Energy Health* **2010**, *5*, 12–19.
28. Niemz, M.H. *Laser–Tissue Interactions: Fundamentals and Applications*, 3rd ed.; Springer: Berlin/Heidelberg, Germany, 2007; ISBN 978-3-540-72191-8.
29. Boulnois, J.-L. Photophysical Processes in Recent Medical Laser Developments: A Review. *Lasers Med. Sci.* **1986**, *1*, 47–66. [[CrossRef](#)]
30. Oraevsky, A.A.; Jacques, S.L.; Tittel, F.K. Determination of tissue optical properties by piezoelectric detection of laser-induced stress waves. *Proc. SPIE* **1993**, *1882*, 86–101.
31. Oraevsky, A.A.; Esenaliev, R.O.; Jacques, S.L.; Tittel, F.K.; Benov, L. Laser optoacoustic tomography for medical diagnostics: Principles. *Proc. SPIE* **1996**, *2676*, 22–31.
32. Wang, L.V.; Wu, H.-I. *Biomedical Optics: Principles and Imaging*; Wiley-Interscience: Hoboken, NJ, USA, 2007; ISBN 978-0471743040.
33. Yao, D.K.; Zhang, C.; Maslov, K.; Wang, L.V. Photoacoustic measurement of the Grüneisen parameter of tissue. *J. Biomed. Opt.* **2014**, *19*, 017007. [[CrossRef](#)]
34. Esenaliev, R.O. Optoacoustic monitoring of physiologic variables. *Front. Physiol.* **2017**, *8*, 1030. [[CrossRef](#)]
35. Feynman, R.P.; Leighton, R.B.; Sands, M. *The Feynman Lectures on Physics: The Flow of Dry Water*; California Institute of Technology: Pasadena, CA, USA, 1964; Volume II, Chapter 40; Available online: https://www.feynmanlectures.caltech.edu/II_40.html (accessed on 25 February 2025).
36. Palmer, K.F.; Williams, D. Optical properties of water in the near infrared. *J. Opt. Soc. Am.* **1974**, *64*, 1107–1110. [[CrossRef](#)]
37. Aria, A.B.; Chen, L.; Silapunt, S. Erythema Ab Igne from Heating Pad Use: A Report of Three Clinical Cases and a Differential Diagnosis. *Cureus* **2018**, *10*, e2635. [[CrossRef](#)] [[PubMed](#)] [[PubMed Central](#)]

Disclaimer/Publisher’s Note: The statements, opinions and data contained in all publications are solely those of the individual author(s) and contributor(s) and not of MDPI and/or the editor(s). MDPI and/or the editor(s) disclaim responsibility for any injury to people or property resulting from any ideas, methods, instructions or products referred to in the content.